Research Article

Journal of PeptideScience

Received: 18 March 2011 Revised: 14 September 2011 Accepted: 15 September 2011 Published online in Wiley Online Library

(wileyonlinelibrary.com) DOI 10.1002/psc.1425

Solution structure by nuclear magnetic resonance of the two lantibiotics 97518 and NAI-107

Francesca Vasile,[a]* Donatella Potenza,[a] Barbara Marsiglia,[b] Sonia Maffioli[c] and Stefano Donadio[c]

Lantibiotics 97518 and NAI-107, produced by the related genera *Planomonospora* and *Microbispora* respectively, are members of a family of nisin-related compounds. They represent promising compounds to treat infections caused by multi-resistant Gram-positive pathogens. Despite their similar structure and a similar antibacterial spectrum, the two lantibiotics exhibit significant differences in their potency. To gain an insight into the structure–activity relationships, their conformational properties in solution are determined by NMR. After carrying out an NOE analysis of 2D ^{1}H NMR spectra, high-resolution 3D structures are determined using molecular dynamics simulations. Copyright © 2011 European Peptide Society and John Wiley & Sons, Ltd.

Keywords: lantibiotic; Nuclear Magnetic Resonance; dynamic simulation; 3D structure

Introduction

Lantibiotics, shortcut for 'lanthionine-containing antibiotic', are small (19–39 amino acids), gene-encoded posttranslationally modified peptides that contain one or more lanthionine (Lan) or methyllanthionine (MeLan) residues. Lan formation involves the dehydration of serine and threonine residues to form 2,3-didehydroalanine (Dha) and (*Z*)-2,3-didehydrobutyrine (Dhb), respectively. This is followed by the regiospecific and stereospecific intramolecular addition of a cysteine thiol onto Dha or Dhb to generate the cognate thioether linkages. When Dha and Dhb residues react with the thiol group of a cysteine residue during the formation of Lan and MeLan residues, they yield D-isomers [1,2]. In addition to (Me)Lan, Dha, or Dhb residues, lantibiotics may undergo other posttranslational modifications, resulting in additional nonproteinogenic amino acids such as the unsaturated Lan derivative *S*-amino vinyl-D-cysteine (AmVinCys).

Recently, the traditional classification [3] based on the topology of the Lan rings has been superseded by a new classification that places lantibiotics into four classes according to the relatedness of the Lan-generating enzymes [4]. Nisin is the prototype of class I lantibiotics, whereas mersacidin and actagardine are typical examples of class II. Despite differences in shape and primary structure, both nisin-type and mersacidin-type lantibiotics interact with the membrane-bound peptidoglycan precursor lipid II [5]. The lantibiotic 97518 (also known as planosporicin) and NAI-107 (also known as 107891 or microbisporicin) (Figure 1) represent newly discovered molecules that, in contrast to most nisin-related compounds, which are produced by strains belonging to the phylum Firmicutes, are produced by the Actinobacteria genera *Planomonospora* and *Microbispora*, respectively. Of the two, NAI-107 is among the most potent antibacterial lantibiotics, covering most Gram-positive pathogens and showing good efficacy in experimental models of infection [6]. It is produced as a complex of two structurally related 24-amino acid variants (A1, 2246-Da; and A2, 2230-Da), which differ in proline-14 being mono-hydroxylated (in variant A2) or bis-hydroxylated (in variant A1). In addition, NAI-107 possesses a 5-chloro-trypthopan, a posttranslational modification previously not reported in lantibiotics. The 1–11 N-terminal sequence is similar to those of nisin, subtilin, epidermin and gallidermin, where it has been demonstrated to be critical for binding to the lipid II pyrophosphate region. The C-terminal ring of NAI-107 is nearly identical to those of epidermin and gallidermin [7,8].

The lantibiotic 97518 was initially reported as a 2194-Da, 24-aa peptide with five thioether bridges and arbitrarily assigned to the mersacidin and actagardine class [9,10]. Maffioli *et al.* [11] demonstrated, through MS and NMR spectroscopy and genome sequencing, its close relatedness to NAI-107, with an identical arrangement of thioether bridges and only six amino acid differences (positions 1, 4, 6, 14, 19 and 22) in the primary structure (Figure 1). Further posttranslational modifications occur only on NAI-107. As a consequence of this structural revision, 97518 is clearly a member of the nisin class of lantibiotics.

* *Correspondence to: Francesca Vasile, Organic and Industrial Chemistry Department, University of Milano, Milan, Italy. E-mail: francesca.vasile@unimi.it*

a *Organic and Industrial Chemistry Department, University of Milano, Milan, Italy*

b *Merck Serono, Ivrea, Italy*

c *New Anti-Infectives Consortium Scrl, Milan, Italy*

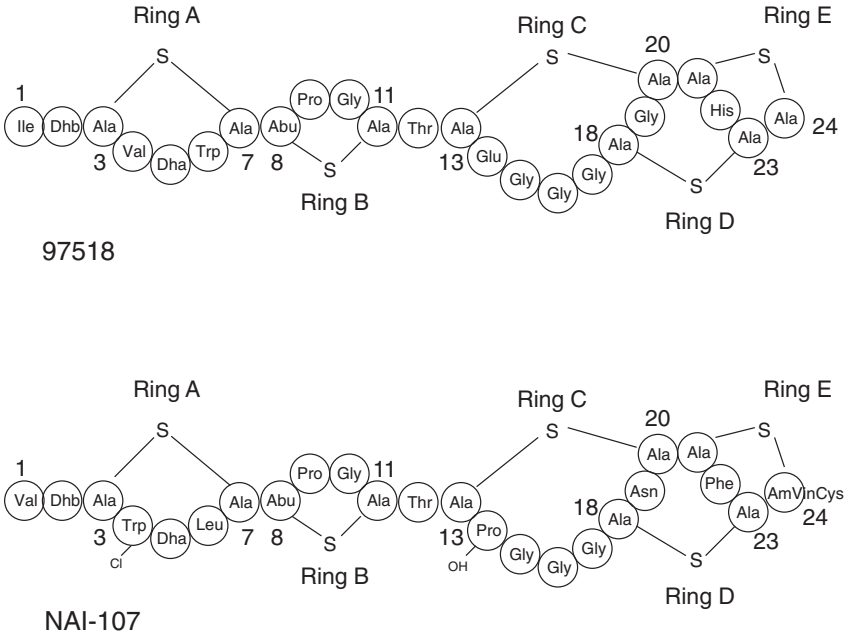

Figure 1. Amino acid sequences and thioether connections of lantibiotics 97518 e NAI-107.

The lesser antibiotic activity of 97518 with respect to NAI-107 [9] must result from subtle differences in their structures because both molecules possess similar amino acid sequences with identical thioether linkages. In addition to their key role in determining the covalent structure of lantibiotics, NMR techniques can provide information on the 3D structure of these complex peptides, allowing conformational analysis for structure–activity relationship studies [12–15].

We report the application of NMR techniques in combination with molecular dynamics simulations to determine the 3D structure of the lantibiotics 97518 and NAI-107.

Materials and Methods

Lantibiotics 97518 and NAI-107 were obtained and purified as reported in refs [9,10].

The samples were prepared dissolving the following: (i) 6.1 mg of 97518 (6 mM) in 60 µl CD_3CN + 400 µl H_2O with 5% D_2O, adjusted to pH 2 with DCl; and (ii) 5 mg of NAI-107 (3.7 mM) in 200 µl CD_3CN + 400 µl H_2O with 5% D_2O, adjusted to pH 2 with DCl. Homonuclear ^1H and heteronuclear ^1H-^{13}C and ^1H-^{15}N NMR experiments were recorded at 600 MHz on a Bruker Avance spectrometer. For structure determination and thioether bonds assignment, the following spectra were used: TOCSY with a mixing time of 20, 60 and 100 ms, NOESY with a mixing time of 300 and 700 ms, ^1H-^{15}N HSQC (J = 90 Hz), ^1H-^{15}N HSQC-TOCSY, ^1H-^{13}C HSQC (J = 145 Hz) and ^1H-^{13}C HMBC with $J^{1H\text{-}13C} = 8$ Hz for long-range correlation. Spectra were acquired at three different temperatures: 283, 298 and 313 K. The excitation sculpting sequence was used for water suppression. The 97518 H/D exchange experiments was performed at 298 K.

Spectra were analysed with the program XEASY [16].

The complete sequence-specific ^1H resonance assignment was obtained following standard procedures [17].

Molecular dynamics analysis was performed using the program DYANA [18], starting from the integrated NOE peaks. The topologies of Dha, Dhb, the alanyl and 3-methylalanyl (Abu) and AmVinCys moieties of lantibiotics were added to the standard amino acid library. According to the enzymology of thioether bridge formation, the N-terminal residue of each Lan ring was assumed to be in the D-configuration. Thus, also D-Ala and D-Abu were added to the library. To avoid steric repulsion, the bridges were defined as covalent links in sequence files. The thioether bridges were constructed fixing 0.31 Å as upper limit between Cβ and S atoms. The macro CALIBA of DYANA was used to perform a standard calibration of NOE peak volumes, using three different calibration classes: one for NOEs assigned to backbone protons, one for NOEs assigned to the more flexible side-chain protons and one for NOEs assigned to methyl groups.

DYANA calculations were started from 100 conformations, randomly generated from a flat distribution of dihedral angles (whereas angles and bond lengths are kept fixed to standard values). The equations of motion are solved in the space of torsion angles of the molecules with a leapfrog algorithm and are coupled to a thermal bath by means of a Berendsen's thermostat. The simulations lasts for 4000 steps, starting with 1000 steps at a temperature of 9600 K and then annealing to 0 K. At the end of the simulation, 1000 steps of conjugated gradient minimization are performed.

The ten conformers with the lowest residual target function values were analysed, the restraints were reexamined in view of consistent violations and relaxed if necessary. This procedure was repeated until no consistent violations were found in half or more of the structures. The ten structures displaying the minimum potential energy and the lowest number of violations were selected for further analysis. The NOE violations >0.02 nm were checked, and they are intraresidual or sequential contacts. In particular, for 97518, the NOE violations concerned the intraresidual distance of Abu8 and Ala 20 and the sequential Abu8-Pro9. Also in the case of 107891, the NOE violations included the intraresidual Abu 8, Ala 21 and Ala23. However, no NOE violations >0.03 nm were found.

Journal of PeptideScience

Results

NMR Analysis

The sequential assignment and the structural analysis for both peptides were determined at 298 K because at 283 and 313 K, the spectra showed a high overlap among signals.

Lantibiotic 97518

The assignment of the spin systems of 97518 and the analysis of the thioether bridges are reported in Maffioli *et al.* [11]

The sequence of 97518 is Ile-Dhb-Ala-Val-Dha-Trp-Ala-Abu-Pro-Gly-Ala-Thr-Ala-Glu-Gly-Gly-Gly-Ala-Gly-Ala-Ala-His-Ala-Ala.

Resonance signals of backbone amide protons of 97518 show partial protection against hydrogen/deuterium (H/D) exchange. After 22 h at 298 K and pH 2.0, only ten amides are left in the TOCSY spectrum, namely, amides belonging to the following residues: Val4, Trp6, Thr12, Ala13, Glu14, Gly16, Gly17, Ala20, Ala21 and Ala24. A total of 153 NOESY cross-peaks obtained with a mixing time of 700 ms are assigned and integrated, yielding 95 nonredundant constraints (28 intraresidue, 45 short, 14 medium and 8 long-range contacts). The formation of hydrogen bonds and exclusion of solvent from the amide protons are assumed to account for the slow and medium amide exchange rates. The partners of the detected hydrogen bonds are assigned on the basis of preliminary structures obtained by imposing only NOE restraints. The detected ten hydrogen bonds were enforced by 20 distance restraints: the distance between the hydrogen and the acceptor is restrained to 0.2 nm, and the distance between the atom covalently bound to the hydrogen and the acceptor is restrained to 0.3 nm.

Lantibiotic NAI-107

The sequence of NAI-107 is Val-Dhb-Ala-ClTrp-Dha-Leu-Ala-Abu-Pro-Gly-Ala-Thr-Ala-Hyp-Gly-Gly-Gly-Ala-Asn-Ala-Ala-Phe-Ala-AmVinCys. Its complete assignment and the J coupling Hα/HN are reported in Table 1.

Also in this case, the spin systems of the nonproteinogenic amino acids Dha and Dhb and of Trp, Leu, Val and AmVinCys are easily identified. Starting from these residues, the sequential assignment is performed, overcoming the problem of the overlapping signals of Ala and Gly residues. The NOEs β8/β11, β13/α20, HN18/Aromatic22, β21/β24, β21/α24 were identified, consistent with the thioether bonds Ala3-Ala7, Abu8-Ala11, Ala13-Ala20, Ala18-Ala23 and Ala21-AmVinCys24. A total of 186 NOESY cross-peaks obtained with a mixing time of 700 ms are assigned and integrated, yielding 110 nonredundant constraints (37 intraresidue, 52 short, 17 medium and 4 long-range contacts).

Molecular dynamic simulation

Lantibiotic 97518

The statistics of the calculated 97518 solution structures is given in Table 2. The imposed hydrogen bonds are NH4/O19, NH6/O10, NH12/O20, NH16/O14, NH20/O18 and NH24/O22. The formation of hydrogen bonds between residues distance along the sequence indicates a compact folding of the molecule. The ten best conformers display a root-mean-square deviation (RMSD) value of 0.082 ± 0.027 nm (Figure 2). In Figure 2, the thioether bridges are evidenced as structural elements important to determine the folding.

Over 87% (21 of the 24) residues in 97518 are part of one of the five thioether rings, which constitute structurally well-defined elements: ring A is made up of five residues ($_{D}$Ala$_{S}$3-Val4-Dha5-Trp6-$_{S}$Ala7); ring B of four residues ($_{D}$Abu$_{S}$8-Pro9-Gly10-$_{S}$Ala11); and rings C, D and E form three intertwined rings composed of eight ($_{D}$Ala$_{S}$13-Glu14-Gly15-Gly16-Gly17-$_{D}$Ala$_{S}$18-Gly19-Ala$_{S}$20), six ($_{D}$Ala$_{S}$18-Gly19-Ala$_{S}$20-$_{D}$Ala$_{S}$21-His22-Ala$_{S}$23) and four ($_{D}$Ala-$_{S}$21-His22-Ala$_{S}$23-Ala$_{S}$24) residues, respectively.

Ring A. No typical β-turns or γ-turns are found in this Lan ring. The RMSD of the backbone atoms were 0.004 nm, indicating a well-defined structure and slow motion. The amide protons of Val4 and Trp6 are detectable for 22 h during a deuterium exchange experiment, and molecular dynamics suggested that the involved carbonyl oxygen belongs respectively to Gly19 and Gly10. In particular, the NH6/O10 bond allows rings A and B to face each other on parallel planes, whereas the NH4/O19 bond causes a more packed folding of the molecule.

Ring B. This 2-methyl-lanthionine ring forms the most well-defined structural element in 97518. The RMSD of the backbone atoms is 0.001 nm. This ring represents a typical motif of lantibiotics formed by four highly conserved residues that represent a very rigid structure [19–22].

Intertwined rings C, D and E. The RMS deviation of the backbone atoms of ring C is 0.089 nm, indicating a considerable amount of motion, whereas the RMSD of the two smaller rings D and E are respectively 0.025 and 0.005 nm. In each of them, a γ-turn was identified, stabilized by three hydrogen bonds between NH16/O14, NH20/O18 and NH24/O22. No β-turns are found in the molecule.

The overall fold of 97518 is also stabilized by the hydrogen bond between NH12/O20.

It is clear from the ensemble of NMR structures that the region between residues 12–20 displays a greater deviation in the backbone RMSD either because of the lack of structurally relevant NOEs, of a greater flexibility of these regions, or both.

Lantibiotic NAI-107

The statistics of the calculated NAI-107 solution structures is given in Table 3. In this case, we did not perform the hydrogen/deuterium exchange analysis. The ten best conformers display an RMSD value of 0.127 ± 0.069 nm.

As in the case of 97518, 21 of 24 residues are part of one of the five thioether rings, involving the same number of residues. Again, ring B is well-defined (with an RMSD of 0.001 nm), whereas ring C is larger and more mobile. In Figure 3, the structure with the lowest energy is reported indicating the ribbon with its secondary structure elements and the side-chain orientation. The γ-turn between residues 13–15 and a β-turn between residues 8–11 can be easily identified (Figure 3).

Discussion

In this paper, the 3D structures of the lantibiotics 97518 and NAI-107 were calculated from several long-range NOEs. Our calculations show very similar solution conformations for the two molecules, consistent with over 70% sequence similarity and identical thioether bridges. A comparison between the backbones of the lowest-energy structure for each lantibiotic indicates a remarkable overall structural similarity (RMSD 0.478 ± 0.089 nm). The match is particularly good in the following regions: amino acids 3–7 (RMSD = 0.06 nm), amino acids 8–11

Table 1. NMR assignment for NAI-107

Residue	NH	H_α ($J_{\alpha/HN}$)	H_β	H_γ	Others
1. Val	—	4.10	2.37	1.09	
2. Dhb	9.92		6.51	1.86	
3. Ala	7.89	4.68 (5 Hz)	3.28–3.01		
4. Trp	8.24	4.71 (7.7 Hz)	3.43–3.33		10.22(NH) 7.60–7.51 7.27–6.91–6.80
5. Dha	8.64	6.24–5.67			
6. Leu	8.70	4.21	1.85–1.81	1.72	1.04
7. Ala	8.06	4.64	3.09		
8. Abu	8.41	4.1 (10.2 Hz)	3.20	1.25	
9. Pro	—	4.41	2.52	2.17–1.96	3.48–3.08
10. Gly	8.58	4.33–3.74			
11. Ala	7.83	4.17	3.60–2.87		
12. Thr	8.16	4.41 (5.2 Hz)	3.61	1.35	
13. Ala	9.23	4.52	3.44–3.16		
14. OH-Pro		4.27	3.81		
15. Gly	7.94	4.21–3.84			
16. Gly	8.40	4.40–3.60			
17. Gly	8.20	4.22–3.89			
18. Ala	8.82	4.53	3.38–3.17		
19. Asn	9.19	5.00	3.01		
20. Ala	8.76	4.28			
21. Ala	8.08	5.14 (8.9 Hz)	3.21–3.13		
22. Phe	8.78	4.31	3.46–3.14		
23. Ala	9.45	4.15	3.52–2.63		
24. AmVinCys	8.68	7.05 (10.2 Hz)	5.82		

Table 2. Structure statistics of 97518 final structures[a]

DYANA target function (Å^2)	6.59 ±0.06 (6.47. . .6.66)
NOE violations >0.2 Å	4.1 ± 0.2 (3.9. . .4.5)
RMSD, backbone (Å)$^{3-21}$	0.82 ± 0.14 (0.20. . .1.43)
RMSD, backbone (Å)$^{3-11}$	0.05 ± 0.03 (0.02. . .0.14)
RMSD, backbone (Å)$^{18-24}$	0.25 ± 0.19 (0.02. . .0.68)

[a]Average values ± standard deviation for the ten final structures, minimum and maximum values for individual conformers in parentheses.

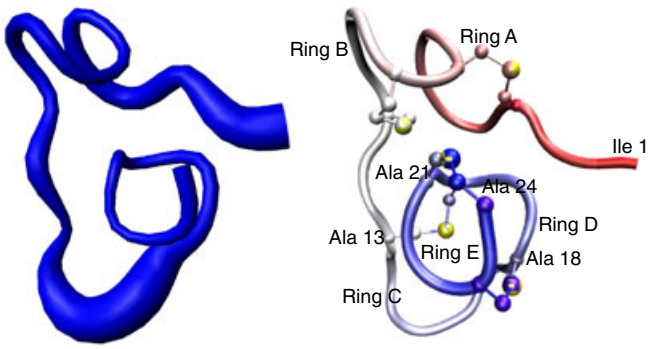

Figure 2. *Sausage representation* (the tube diameter is function of local RMSD) of the best ten structures obtained for 97518 (left) and the structure with the lowest energy (right). The thioether bridges are indicated and the dotted lines represent the most significative NOE contacts.

(RMSD = 0.071 nm) and amino acids 18–24 (RMSD = 0.063 nm). The amino acids 12–18, displaying higher flexibility, has an RMSD value of 0.24 nm.

On the basis of their structure and their function, these molecules are classified as class I lantibiotics. It is generally believed that type A lantibiotics exert their cell-killing action by formation of pores in the cytoplasmatic membrane of target cell [23,24].

As reported in the literature [9,10], the N-terminal portion of 97518 and NAI-107 shows a great similarity with N-terminal (1–11) part of class I lantibiotics (nisin, gallidermin and others) [19–21], and it is crucial for binding to the lipid II pyrophosphate region.

In nisin, the structures of the ring systems are well or reasonably well defined, whereas the structure of the linear peptide segments is less defined. The rings in the N-terminal half of the molecule are part of a structured domain, and the residues Lys22 to Ala28 form a structured domain in the C-terminal half. The structures in the nisin/H,O and nisinIDodPCho systems are somewhat better defined in that the rings A, B and C have similar orientations with respect to each other. For nisin/SDS, only rings A and B have a well-defined relative orientation, whereas the position of ring C relative to ring B is structurally ill characterized [14].

In 97518, we can observe a parallel orientation between rings A and B similar to that observed for nisin. In NAI-107, rings A

Journal of PeptideScience

Table 3. Structure statistics of NAI-107 final structures[a]

DYANA target function (Å^2)	4.20 ±0.13 (3.92. . .4.35)
NOE violations > 0.02 nm	0.49 ± 0.04 (0.41. . .0.54)
RMSD, backbone (nm)$^{3-21}$	0.127 ± 0.069 (0.031. . .0.18)
RMSD, backbone (nm)$^{3-11}$	0.034 ± 0.012 (0.023. . .0.055)
RMSD, backbone (nm)$^{18-24}$	0.049 ± 0.021 (0.008. . .0.064)

[a]Average values ± standard deviation for the ten final structures, minimum and maximum values for individual conformers in parentheses.

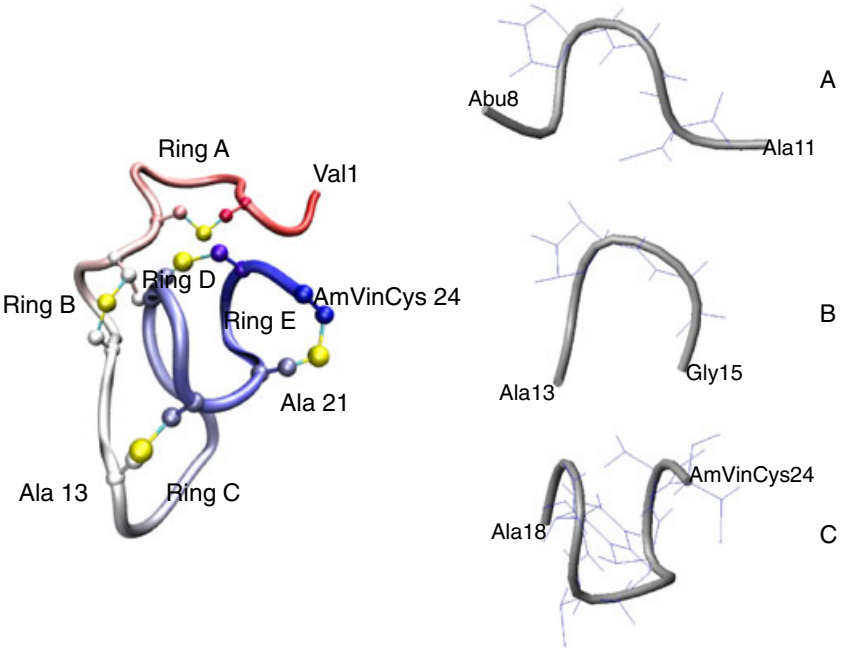

Figure 3. Structure with the lowest energy obtained for NAI-107 (left). On the right, the following motifs are evidenced: ring B (residues 8-11) with the formation of a β-turn (A), the γ-turn formed between residues 13-15 (B) and the ring D between residues 18-24 (C).

and B are not parallel, but in this peptide, ring D and E are on parallel planes.

In the literature [9], it is also reported that the lipophilic nature of Cl-Trp4 of NAI-107 could be important for its affinity to the membrane compartment, but in the N-terminal region, no significative structural variations are evidenced to support this hypothesis.

Both 97518 and NAI-107 act in blocking peptidoglycan (PG) biosynthesis, but NAI-107 shows a higher activity than 97518 against all tested microorganisms (see Table 3 of [9]). As observed in the case of other lantibiotics of the same family (i.e. nisin and gallidermin), the structure of the thioether rings is rigid and well defined. Like in nisin, the region not spanned by thioether linkages is quite flexible [14,19,21], and it may be important for antibacterial activity, allowing lantibiotics to orient properly towards the membrane.

The most important structural difference between 97518 and NAI-107 is in the more flexible region (amino acids 12–18), determined also by two amino acid differences at position 14 (Hyp in NAI-107 and Glu in 97518) and 19 (Asn and Gly, respectively). From the present data on the 3D structures of the two lantibiotics in water solution, only the features of the 12–18 region might relate to differences in bioactivity: this region is well defined in 97518 and more mobile in NAI-107, consistent with the importance of flexibility for interaction with the membrane. It should be noted that 97518 has a negative charge in this region (Glu14) not present in NAI-107, which might also be important for the difference in activity. Further studies are required to understand the features of the two lantibiotics responsible for antibacterial activity.

References

1 Kellner R, Jung G, Horner T, Zähner H, Schnell N, Entian KD, Gotz F. Gallidermin: a new lanthionine-containing polypeptide antibiotic. *Eur. J. Biochem.* 1988; **177**: 53–59.
2 Allgaier H, Jung G, Werner RG, Schneider U, Zähner H. Epidermin: sequencing of a heterodet tetracyclic 21-peptide amide antibiotic. *Eur. J. Biochem.* 1986; **160**: 9–22.
3 McAuliffe O, Ross RP, Hill C. Lantibiotics: structure, biosynthesis and mode of action. *FEMS Microb. Rev.* 2001; **25**: 285–308.
4 Willey JM, van der Donk WA. Lantibiotics: peptides of diverse structure and function. *Annu. Rev. Microbiol.* 2007; **61**: 477–501.
5 Martin NI, Breukink E. Expanding role of lipid II as a target for lantibiotics. *Future Microbiol.* 2007; **2**: 513–525.
6 Jabes D, Brunati C, Candiani G, Riva S, Romano' G, Donadio S. Efficacy of the new lantibiotic NAI-107 in experimental infections induced by MDR Gram positive pathogens. *Antimicrob. Agents Chemother.* 2011. doi: 10.1128/AAC.01288-10
7 Chatterjee MP, Xie L, van der Donk WA, Biosynthesis and mode of action of lantibiotics. *Chem. Rev.* 2005; **105**: 633–684.
8 Bonelli RR, Schneider T, Sahl HG, Wiedemann I. Insights into in vivo activities of lantibiotics from gallidermin and epidermin mode-of-action studies. *Antimicrob. Agents Chemother.* 2006; **50**: 1449–1457.

9 Castiglione F, Lazzarini A, Carrano L, Corti E, Ciciliato I, Gastaldo L, Candiani P, Losi D, Marinelli F, Selva E, Parenti F. Determining the structure and mode of action of microbisporicin, a potent lantibiotic active against multiresistant pathogens. *Chem. Biol.* 2008; **15**: 22–31.
10 Castiglione F, Cavaletti L, Losi D, Lazzarini A, Carrano L, Feroggio M, Ciciliato I, Corti E, Candiani G, Marinelli F, Selva E. A novel lantibiotic acting on bacterial cell wall synthesis produced by the uncommon actinomycete Planomonospora sp. *Biochemistry* 2007; **46**: 5884–5895.
11 Maffioli SI, Potenza D, Vasile F, De Matteo M, Sosio M, Marsiglia B, Rizzo V, Scolastico C, Donadio S. Structure revision of the lantibiotic 97518. *J. Nat. Prod.* 2009; **72**(4): 605–607. DOI: 10.1021/np800794y
12 an den Hooven HW, Fogolari F, Rollema HS, Konings RN, Hilbers CW, van de Ven FJ. NMR and circular dichroism studies of the lantibiotic nisin in non-aqueous environments. *FEBS Lett.* 1993; **319** (1–2): 189–194.
13 Zimmermann N, Jung G. The three-dimensional solution structure of the lantibiotic murein-biosynthesis-inhibitor actagardine determined by NMR. *Eur. J. Biochem.* 1997; **246**(3): 809–819.
14 Van Den Hooven HW, Doeland CC, Van De Kamp M, Konings RN, Hilbers CW, Van De Ven FJ. Three-dimensional structure of the lantibiotic nisin in the presence of membrane-mimetic micelles of dodecylphosphocholine and of sodium dodecylsulphate. *Eur. J. Biochem.* 1996; **235**(1–2): 382–393.
15 Ekkelenkamp MB, Hanssen M, Danny Hsu ST, de Jong A, Milatovic D, Verhoef J, van Nuland NA. Isolation and structural characterization of epilancin 15X, a novel lantibiotic from a clinical strain of Staphylococcus epidermidis. *FEBS Lett.* 2005; **579**(9): 1917–1922.
16 Bartels C, Xia T, Billeter M, Giintert P, Wuthrich K. The program XEASY for computer-supported NMR spectral analysis of biological molecules. *J. Biomol. NMR* 1995; **6**: I–lO.
17 Wuthrich K. *NMR of Proteins and Nucleic Acids*. New York (NY), USA: Wiley-Interscience. 1986. ISBN: 0471119172
18 Guntert P, Mumenthaler C, Wuthrich K. Torsion angle dynamics for NMR structure calculation with the new program DYANA. *J. Mol. Biol.* 1997; **273**: 283–298.
19 Van de Ven FJ, Van den Hooven HW, Konings RN, Hilbers CW. NMR studies of lantibiotics. The structure of nisin in aqueous solution. *Eur. J. Biochem.* 1991; **202** (3): 1181–1188.
20 van Leeuwenhoek A Structures of lantibiotics studied by NMR. *Biomedical and Life Sciences.* 1996; **69** (2): 99–107. DOI: 10.1007/BF00399415
21 Freund S, Jung G, Gutbrod O, Folkers G, Gibbons WA, Allgaier H, Werner R. The solution structure of the lantibiotic gallidermin. *Biopolymers* 1991; **31**(6): 803–811.
22 Smith L, Zachariah C, Thirumoorthy R, Rocca J, Novák J, Hillman JD, Edison AS. Structure and dynamics of the lantibiotic mutacin 1140. *Biochemistry* 2003; **42**: 10372.
23 van De Ven FJM, Jung G, Structures of lantibiotics studied by NMR. *Antonie Van Leeuwenhoek*, 1996; **69**: 99.
24 Kodani S, Hudson ME, Durrant MC, Buttner MJ, Nodwell JR, Willey JM. The SapB morphogen is a lantibiotic-like peptide derived from the product of the decelopmental gene *ramS* in *Streptomyces coelicolor*. *P.N.A.S.* 2004; **101**: 11448.

